

Laser Frequency Stabilization for GRACE-II

W. M. Folkner, G. deVine, W. M. Klipstein,
K. McKenzie, D. Shaddock, R. Spero, R. Thompson,
D. Wuchenich, N. Yu
Jet Propulsion Laboratory, California Institute of
Technology
4800 Oak Grove Drive
Pasadena, CA 91109

M. Stephens, J. Leitch, M. Davis, J. deCino, C. Pace,
R. Pierce
Ball Aerospace and Technologies Corporation
PO Box 1062
Boulder, CO 80306-1062

Abstract—The GRACE mission monitors changes in the Earth’s gravity field by measuring changes in the distance between spacecraft induced by that changing field. The distance variation is measured with a microwave ranging system with sub-micron accuracy. The ranging measurement accuracy is limited by the signal-to-noise ratio and by the frequency stability of the microwave signal referenced to an ultra-stable oscillator (USO). For GRACE-2 a laser ranging system is envisioned with accuracy better than the GRACE microwave ranging system. A laser ranging system easily provides an improved signal-to-noise ratio over the microwave system. Laser frequency stability better than the GRACE USO stability has been demonstrated in several laboratories using thermally stabilized optical cavities. We are developing a space-qualifiable optical cavity and associated optics and electronics for use on GRACE-2 to provide a stable frequency reference for the laser ranging system. Two breadboard units have been developed and tested for performance and ability to survive launch and orbit environments. A prototype unit is being designed using lessons learned from tests of the breadboard units.

I. INTRODUCTION

The GRACE mission [1] has been monitoring variations in the Earth’s gravity field since launch in 2005. A microwave ranging instrument is used to measure changes in distance between two dedicated spacecraft in polar circular orbits at an altitude of about 450 km with separation of about 200 km [2]. An accelerometer on each spacecraft is used to measure atmospheric drag forces to remove the drag signature from the ranging data [3]. The spacecraft orbits have a 30-day repeat cycle, and a new gravity field is determined each month. The GRACE system accuracy is sufficient to determine a change in mass equivalent to a volume of water with depth 1 cm over a radius of about 400 km [4].

The GRACE microwave ranging instrument accuracy is limited primarily by the signal-to-noise ratio and by microwave frequency stability derived from an ultra-stable oscillator [5]. The other significant source of system noise is the accuracy with which atmospheric drag and other non-gravitational forces are calibrated with the accelerometer. A future GRACE-2 mission may achieve significantly improved system accuracy by replacing the microwave ranging instrument with a laser ranging instrument. Because of the shorter wavelength a laser ranging system can easily provide a higher signal-to-noise ratio

than the GRACE microwave ranging system [6]. Frequency stability of a laser locked to a thermally stabilized cavity has been shown in laboratory experiments to be better than the GRACE USO stability [7,8]. Improved calibration of non-gravitational forces may be achieved through use of drag-free operation, such as currently being developed for the LISA mission with a performance demonstration on the LISA Pathfinder mission [9]. In the presence of atmospheric drag the performance of the drag-free control is expected to have more acceleration noise than for the LISA case [10] but should still be capable of two to three orders of magnitude better performance than the GRACE accelerometer. With improved instrumentation GRACE-II may be limited by aliasing of under-sampled signatures rather than by system noise [11]. Other mission architectures with either different types of orbits [12] or more than one pair of spacecraft [13] may provide better sampling to give improved overall gravity field accuracy.

The research described below is primarily aimed at developing a thermally stabilized optical cavity subsystem suitable for launch and operation on a future mission. An optical subsystem for directing the laser beam for the range measurement has been developed previously [6]. A technology demonstration of a laser ranging instrument is being considered for a recently announced GRACE Follow-on mission. Such a demonstration would require some compromises in the instrument architecture to work around the microwave ranging instrument that will be the primary instrument for the Follow-on mission. A conceptual layout of the technology demonstration is described here to illustrate the application of the laser frequency stability research being performed and some of the issues remaining to be addressed. We also describe the laser stabilization subsystem in development and give current results.

II. LASER RANGING ARCHITECTURE FOR TECHNOLOGY DEMONSTRATION

A. Laser beam path

Because the calibration of non-gravitational forces is crucial for GRACE, the reference mass for an accelerometer is located as close to the spacecraft center of mass as possible. The microwave ranging instrument is designed such that the measurement is as close as possible to the direct line between the reference masses on the two spacecraft to minimize noise

due to pointing fluctuations and thermal changes in the distance between the microwave antenna phase center and the reference mass. With a laser ranging system, it is practical to reflect the laser beam directly off the reference mass, which is the approach taken for the LISA/LISA Pathfinder system designs and assumed for the previous development of a laser ranging optical system for GRACE-II.

Like the microwave ranging instrument, the laser ranging instrument is intended to measure change in range as a function of time rather than absolute range. The instrument is based on transmission of a continuous signal with the wavelength locked to the frequency reference. In the case of the microwave instrument, the carrier phase of the signal received from the other spacecraft is measured with respect to the local frequency reference. The phase measurements on each spacecraft are processed in the data center to determine the round-trip range. The range measurement for the first range point is ambiguous by an arbitrary integer number of wavelengths. Thereafter the phase is continuously tracked and range changes determined to a fraction of the wavelength, which is 1 cm. For the laser ranging instrument it is not practical to measure the laser carrier phase separately at each spacecraft as was done for the microwave instrument. Instead one spacecraft laser is locked to its frequency reference while the laser at the second spacecraft is locked to the laser received from the first spacecraft.

Figure 1 shows the internal configuration of the GRACE spacecraft. For the technology demonstration, the location of the microwave instrument and propellant tanks interfere with the optical beam path for laser ranging. Instead the current concept is based on using three mirrors to create a corner cube arrangement centered on the accelerometer reference mass, as shown in Figure 2. The laser beam would make a roughly rectangular path, or racetrack, from one spacecraft to the other and back [14]. This configuration gives a round-trip distance measurement which is, to first order, insensitive to attitude variations of the spacecraft.

An entire corner-cube is not needed since the spacecraft pointing will be controlled within a few milliradian. Instead, a fixture will hold three small mirrors at the locations needed to cover the small range of points that the laser needs to reflect off to cover the range dictated by the spacecraft attitude control.

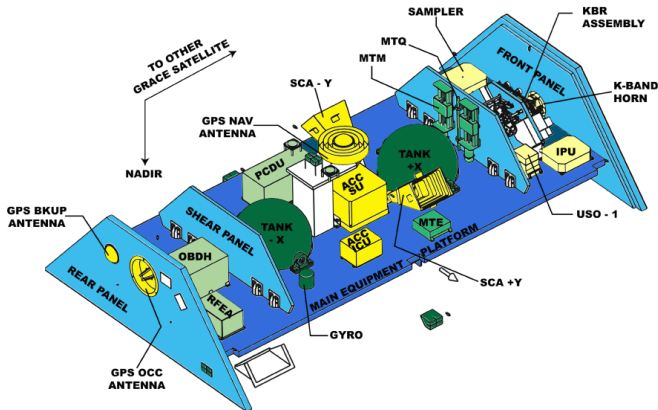


Figure 1. Internal configuration of GRACE spacecraft

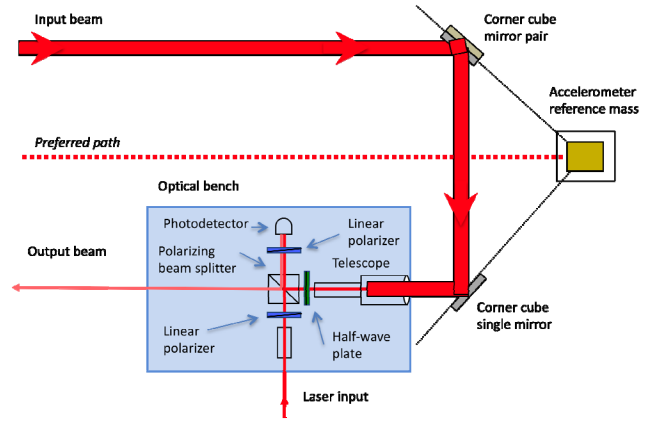


Figure 2. Racetrack optics configuration on one spacecraft

Compared with the preferred path with light directly traveling between reference masses on each spacecraft, the racetrack has additional potential measurement noise from several sources, such as roughness in the surface of the mirrors which causes change in path length with change in attitude, and thermal distortions of the fixture holding the mirrors.

B. Laser beam pointing

The GRACE spacecraft pointing control is designed to meet the requirements of the microwave ranging instrument. The pointing variations are about 1 milliradian root-mean-square. Examples of on-orbit pointing errors are shown in Figures 3 and 4. The spacecraft attitude is measured with star trackers with accuracy $\sim 10 \mu\text{radian}$. The pointing variation results from the use of cold gas thrusters combined with magnetic torque rods for spacecraft attitude control, giving fairly coarse actuation resolution. Reaction wheels, which would provide more precise attitude control, are not used on GRACE to avoid possible issues of vibrations affecting the precision accelerometer.

For the laser ranging instrument it is desirable to have better pointing accuracy to reduce secondary measurement noise terms. For GRACE-II it is likely that electrical propulsion will be used to control spacecraft attitude and possibly also for drag compensation. It is likely that the propulsion system will allow attitude control accuracy to approach the star tracker measurement accuracy. The laser ranging instrument can also provide a measurement of the direction to the other spacecraft, by measuring the difference of the phase of the laser received from the other spacecraft across four quadrants of a photodetector. The accuracy of the pointing signal from the laser ranging instrument might be more accurate than from the star trackers, depending on the specific design parameters.

For the technology demonstration on the GRACE Follow-on mission, the spacecraft pointing stability is likely to be slightly better than for GRACE due to refinement of the control algorithms. The laser ranging instrument design may need to have a more stable pointing capability than the spacecraft provides. One approach to implementing a pointing capability is to mount the laser optical bench on a pivot and actuate it in yaw and pitch using two linear motion actuators. The resulting motion can affect the accelerometer through the gravitational

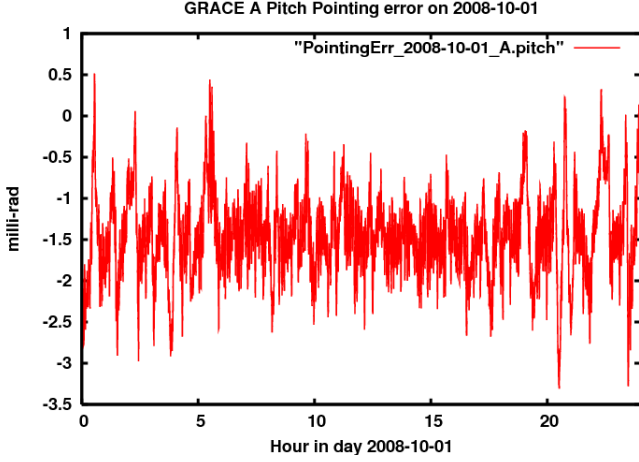


Figure 3. Example GRACE pointing variation in pitch

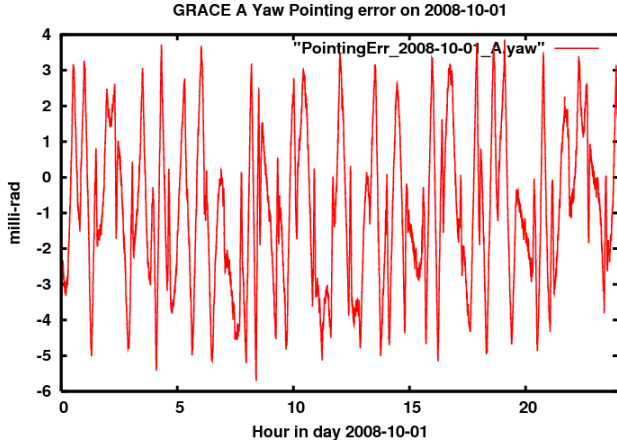


Figure 4. Example GRACE pointing variation in yaw

effect of the motion of the bench relative to the rest of the spacecraft. Taking the x direction to be the direction to the other spacecraft, and the z direction to be the direction perpendicular to the laser racetrack, the optical bench may notionally be considered as two point masses of order 1 kg each located at approximate locations of (0.6m, 0.5m, 0.1m) and (0.4m, 0.5m, 0.1m) relative to the spacecraft center of mass, where the accelerometer reference mass is located. A rotation of 1 milliradian about the z-axis (yaw) will cause an acceleration on the reference mass of less than $2.5 \times 10^{-14} \text{ m/s}^2$ in any direction. A rotation about the y-axis (pitch) produces a smaller acceleration. The accelerometer accuracy is about 10^{-10} m/s^2 , so motion of the optical bench appears to be an acceptable approach.

C. Leading measurement noise source comparison

The major system measurement noise sources for GRACE are the microwave thermal noise, the microwave USO noise, and the accelerometer noise. Figure 5 is a plot of the power spectral density of the resulting noise on the measured one-way range-change, which shows the frequency dependency of each effect. We here concentrate on signal frequencies of 10 mHz to 100 mHz which, for an orbital velocity of $\sim 7 \text{ km/s}$, correspond to spatial scales of 70 km to 700 km on the surface of the Earth.

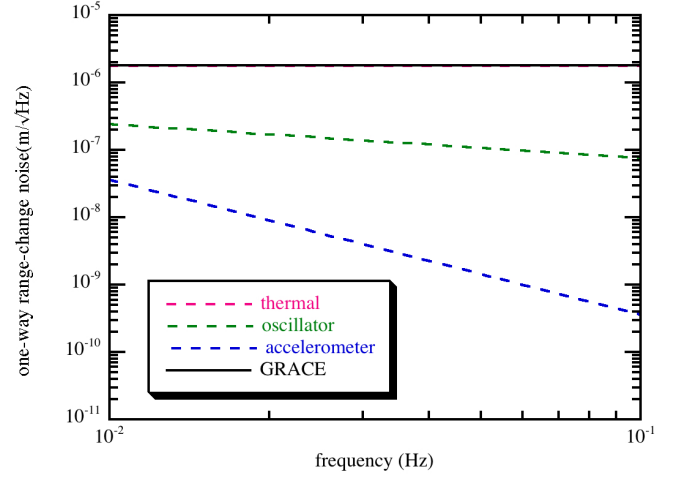


Figure 5. GRACE one-way range-change noise power spectral density

These spatial scales are the main target for improvement with the laser ranging instrument.

For the laser ranging system the noise terms corresponding to microwave thermal noise and USO noise are shot noise and laser frequency noise. We assume for now that the accelerometer noise for the GRACE Follow-on mission is the same as for GRACE. The laser frequency noise is taken as $30 \text{ Hz}/\sqrt{\text{Hz}}$ which is the goal for the stabilization system under development described in Section III. Lacking an optimized design of optics for the racetrack, we consider here the use of the previously developed interferometric ranging transponder (IRT) optics [6] used in the racetrack configuration.

The relevant optical parameters for the racetrack configuration are given in Table 1. In the case of an on-axis configuration, this design includes an optical bench with 1 mm diameter laser beam on the bench and output in the direction of the reference mass and a 12 mm diameter telescope used to transmit to, and receive from, the other telescope. Used in the racetrack configuration, the 1 mm diameter beam is used to transmit to the other spacecraft and the 12 mm telescope is used to receive the signal from the other spacecraft routed through the corner-cube mirrors. This gives considerably lower signal levels for a given laser power than in the on-axis configuration but can still give suitable performance for the technology demonstration as shown below.

TABLE I. INTERFEROMETRIC RANGE TRANSPONDER OPTICAL PARAMETERS IN RACETRACK CONFIGURATION

Parameter	Value	Units
Spacecraft separation	200	km
Laser power	200	mW
Laser transmission efficiency to bench	30	%
Laser wavelength	1064	nm
Optical bench receive efficiency	50	%
Beam diameter on optical bench	0.001	m
Transmit telescope magnification	1	
Receive telescope diameter	0.012	m
Photodetector responsivity	0.2	A/W

There are some advantages of using a smaller transmit beam diameter. The wider diffraction-limited beam is comparable to the GRACE spacecraft pointing noise, which can simplify initial signal acquisition, and the wider beam gives smaller noise due to pointing jitter, which can relax performance requirements on the laser beam pointing subsystem.

The laser ranging accuracy limit from signal to noise is dominated by the photon shot noise, which is related to the received power P_r . The received power is given by

$$P_r \approx \varepsilon_r \frac{D^2}{(2\theta_d L)^2} \varepsilon_t P_L = \varepsilon_r \left(\frac{\pi}{2\lambda}\right)^2 \left(\frac{D^2 (G\omega_0)^2}{L^2}\right) \varepsilon_t P_L \quad (1)$$

where ε_r is the optical efficiency of the receive bench, D is the receive telescope aperture diameter, θ_d is the divergence half-angle of the beam, L is the distance between spacecraft, P_L is the laser power, ε_t is the transmission optical efficiency, λ is the laser wavelength, G is the transmit telescope magnification, and ω_0 is the beam radius on the optical bench. With the instrument parameters in Table 1 and a spacecraft separation of 200 km, the received power is 266 pW.

On the optical bench the received light is mixed with light from the laser on the receiving spacecraft with power P_o using a beam splitter and imaged onto a photodetector. This produces a current I proportional to the square of the received and local electric field amplitudes, which is related to the power levels and the cosine phase difference ϕ between the incoming and local laser, given by.

$$I = R[P_r + P_o + 2\sqrt{P_r}\sqrt{P_o} \cos(\phi)] \quad (2)$$

where R is the photodetector responsivity (in units of A/W). The noise current power spectral density S_i due to photon shot noise is proportional to the current. Since the power of the local laser on the photodiode is generally much larger than the received power, the shot noise (in units of A/ $\sqrt{\text{Hz}}$) is given by

$$\sqrt{S_i} = \sqrt{2eI} \approx \sqrt{2eRP_o} \quad (3)$$

where e is the charge of an electron. The range change measurement noise is given by the wavelength times the noise in the measurement of the phase difference. The power spectral density of the phase noise (in units of radians/ $\sqrt{\text{Hz}}$) is given by

$$\sqrt{S_\phi} = S_i / I_s = \sqrt{e/(2RP_r)} \quad (4)$$

where I_s is the part of the current proportional to the phase difference.

Figure 6 shows the noise on the one-way range-change for the shot noise calculated above along with the laser frequency noise and the accelerometer noise. Other noise sources need to be considered, including wave-front fluctuations due to pointing variations, variations in beam path on the reflecting

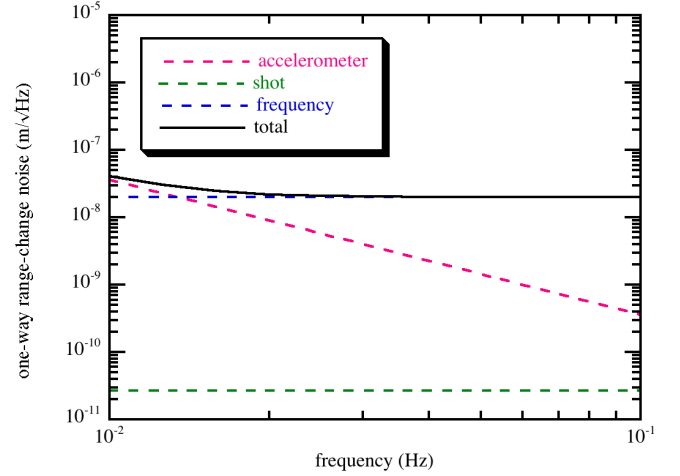


Figure 6. Example GRACE follow-on one-way range-change noise power spectral density

optics due to pointing variations (beam walk), thermally induced variations in the positions of the optics, etc. Those should be smaller than the major sources shown here but are deferred to a more detailed design analysis.

III. LASER FREQUENCY STABILIZATION DESIGN

A common means to provide a stable laser frequency is to form an optical cavity by attaching mirrors to the ends of a ‘spacer’ made of a material of with a very low thermal expansion coefficient. The laser frequency is locked to the length of the cavity by comparing the laser output frequency with light which has resonated in the cavity. Glasses such as zerodur or ULE have thermal expansion coefficients of order $3 \times 10^{-8}/\text{K}$. The optical cavity can be insulated from external sources of heat, so that temperature fluctuations experienced by the cavity are reduced.

The laser frequency stabilization goal adopted for this development is a frequency noise power spectral density of 30 Hz/ $\sqrt{\text{Hz}}$ over the frequency range of interest, 10 mHz to 100 mHz. This performance has also been considered for the LISA instrument design. Performance is practically limited by brownian motion noise of the spacer [15] to about one order of magnitude lower than the adopted goal. Performance approaching the brownian-noise limit has been achieved in laboratories [7,8]. We have adopted a less ambitious goal to ensure that the system can survive launch vibrations and on-orbit thermal extremes.

The cavity is based on a design available from Advanced Thin Films and used successfully in laboratory tests. The spacer is made out of ULE. The spacer cross-section tapers from the middle towards each end and is designed to be mounted vertically to reduce distortions due to ground vibration. While mounting in the center is not as important for use in space, the vertical mounting has potentially improved performance when testing prior to launch. The length of the spacer is 77.5 mm. End mirrors were attached using optical contacting. The mirror coating was chosen to achieve a finesse of about 10,000. This is lower than typical for laboratory use, but eases requirements on alignment of the injection optics,

which must survive launch and the space environment. The cavity is mounted from a flange by titanium flexures bonded to the spacer, as shown in Figure 7. The flange is part of a titanium vacuum enclosure which serves as the first stage of a two-stage thermal isolation enclosure. It provides a controlled vacuum environment to reduce fluctuations of refraction within the cavity and eliminates convection between the cavity and the vacuum enclosure. Laser light is injected into the cavity via a single-mode optical fiber. An optical bench made out of zerodur contains optics to match the light from the output of the fiber into the cavity. The optical bench is also made of zerodur and is mounted to the cavity using titanium flexures. A quadrant photodetector is mounted to the vacuum flange to allow the alignment of the injection optics to be checked using light transmitted through the cavity. Light output from the cavity is rotated via a quarter-wave plate and mixed with the input light from the laser with a polarizing beam-splitter before exiting the vacuum enclosure via a multimode fiber.

The second stage of the two-stage thermal isolation design is formed by an outer aluminum enclosure from which the vacuum enclosure is suspended by titanium flexures, as shown in Figure 8. The current breadboard implementation includes a vacuum valve on the bottom for testing purposes. During a re-design planned at the completion of tests of the breadboard system, the valve will be removed to reduce volume and mass for the prototype unit. An ion gauge is mounted on the outside of the cavity vacuum flange. Heaters and temperature sensors are attached near the top and the bottom of the outer aluminum enclosure to control the temperature of the ends of the enclosure.

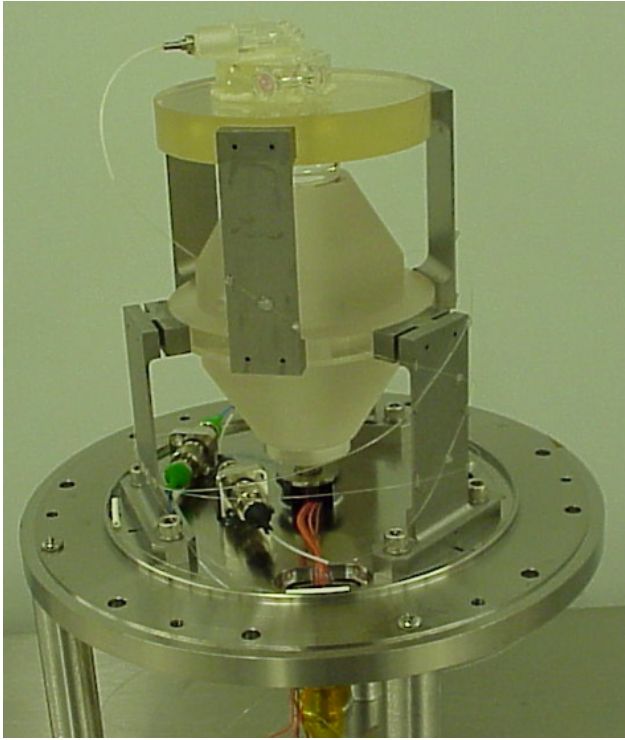


Figure 7. Laser frequency stabilization cavity and optical bench mounted on vacuum flange

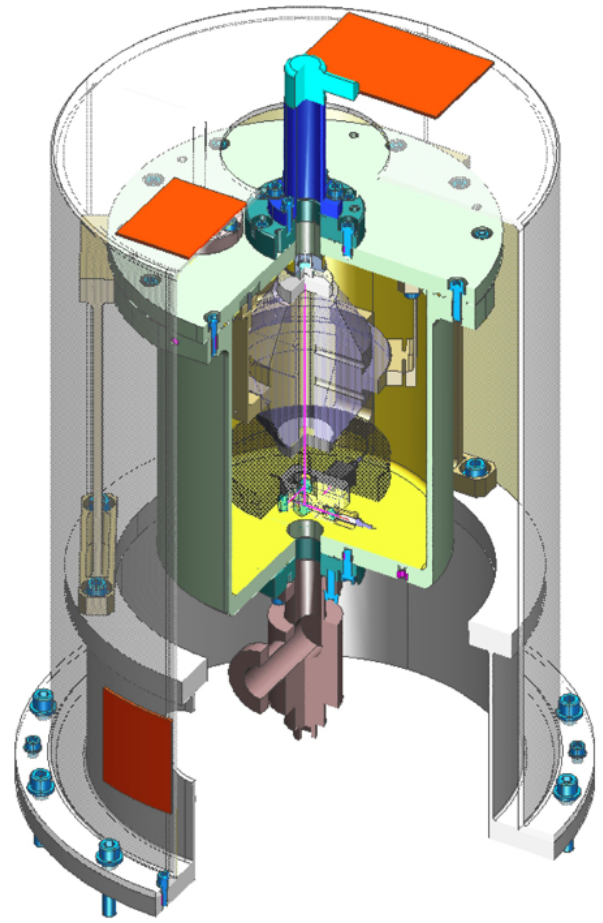


Figure 8. Cut-away view of laser frequency stabilization cavity assembly

IV. LASER FREQUENCY STABILIZATION TESTING

A. Frequency stability test configuration

In order to evaluate the frequency stability of the cavity/enclosure assembly, a laser was locked to each of two breadboard assemblies and the frequency of the two stabilized lasers was compared. The cavities had measured free-spectral ranges (FSR) of 1.9377 GHz and 1.9335 GHz, respectively, and measured linewidths of approximately 150 kHz, equating to a finesse of approximately 13000. The two cavity assemblies were installed in separate outer vacuum enclosures placed on the same optical bench approximately 1 m apart. Neodymium:YAG lasers were employed with 500 mW output power at wavelength 1064 nm. The lasers use a non-planar ring crystal (NPRO) [16] by which the frequency can be adjusted using a piezo-electric crystal (PZT) bonded to the laser crystal and by changing the temperature of the laser crystal. The output of each laser was split, attenuated and fiber-coupled into the vacuum can containing the cavity, with an incident power of a few mW.

The outputs of the two stabilized lasers were interfered on a free-space beam-splitter. The resulting beat note was detected with a high-bandwidth photoreceiver. The frequency difference

between the lasers locked to the independent cavities was of the order of hundreds of MHz to GHz (depending on which longitudinal cavity mode and/or which laser-cavity combination was selected). The beat signal was mixed down with a function generator and double-balanced analog mixer. This placed the frequency of the beat note within the 20 MHz bandwidth of high-accuracy phase measurement electronics developed originally for GRACE-II [17] and further developed for the LISA instrument [18]. The beat note was typically mixed down to 5 MHz, with the phase measurement electronics tracking the phase of this signal and recording data at 100 Hz. The recorded phase was differentiated to produce frequency data for stability analysis.

B. Pound-Drever-Hall locking

Initial testing focused on employing the Pound-Drever-Hall (PDH) locking technique [19]. The laser light into the cavity was phase modulated. The modulation frequency of ~ 5 MHz was applied using fiber-coupled electro-optical modulators driven by external function generators. Light output from the cavity was interfered with input light reflected off the cavity input mirror. The PDH test configuration is shown in Figure 9.

The photoreceiver signal was digitized using an analog-to-digital converter and processed using a control algorithm implemented on a field-programmable gate-array (FPGA) which estimated the error signal and generated the control signals to adjust the laser frequency [20]. The correction signals were fed back to both the PZT (fast) and temperature (slow) inputs of the laser via the FPGA and a digital-to-analog converter, for long-term laser locking control to the cavity.

Typical laser frequency stability results are shown in Figure 10. The frequency stability achieved does not quite meet the performance goal, though is as good as the GRACE USO at 10 mHz and better than the GRACE USO at 100 mHz. The frequency noise showed evidence of stray interference, which was not unexpected given the use of fibers for the getting light into and out of the cavity.

C. Low modulation frequency locking

The coupling of the spurious interference noise into the cavity locking signal depends on the amplitude of the stray interferometer and on the modulation frequency used for the locking signal. The free spectral range of the stray interferometer was estimated to be tens of MHz. Reducing the modulation frequency to well below the free spectral range of

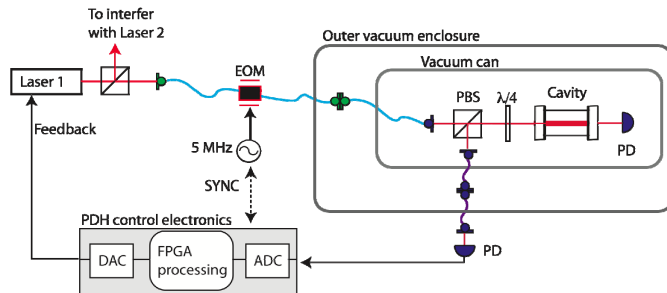


Figure 9. Test configuration using the Pound-Drever-Hall technique with reflected light

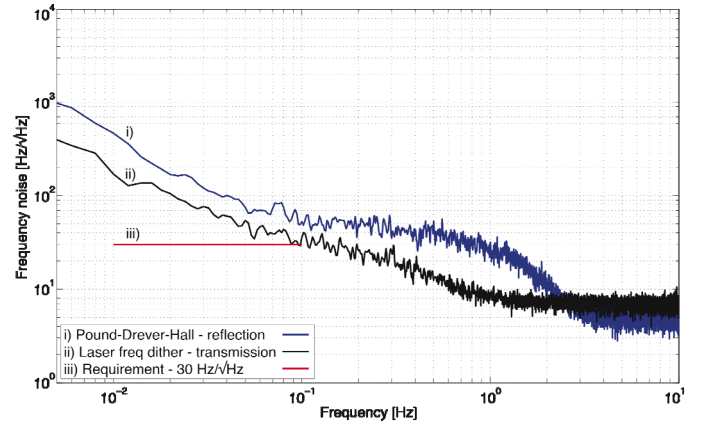


Figure 10. Noise spectra obtained from PDH on reflection and dither locking on transmission.

the stray interferometer should result in unwanted sidebands giving a smaller differential phase response.

For tests with low modulation frequency, the laser frequency was modulated with a ‘dither’ in the range of 50 kHz to 150 kHz using the PZT crystal bonded to the NPRO laser crystal. Using the PZT eliminated the fiber-coupled electro-optical modulator as a potential source of interference, and reduced the number of elements needed. Light transmitted through the cavity onto the photodetector inside the cavity vacuum enclosure was used for locking. Using transmitted rather than reflected light bypassed the multi-mode optical fiber used for reflected light in the Pound-Drever-Hall technique. The configuration used for the low-frequency locking is shown in Figure 11.

Laser frequency modulation introduces amplitude modulation at the modulation frequency. For cavity line-width $\nu_L = 150$ kHz, the modulation amplitude is on the order of or less than ν_L , and the observed (undesired) normalized intensity modulation is $\Delta I = 1 \cdot 10^{-6}$. This has the effect of shifting the lock point by approximately $\nu_L \cdot \Delta I = 0.15$ Hz, which is a negligible amount.

Another potential disadvantage of low-frequency modulation is intensity noise at the modulation frequency. The lasers exhibit more intensity noise at lower frequency. Figure 12 shows the measured intensity noise $I(f)$ at frequencies low enough to use laser PZT modulation. For modulation frequency $f > 20$ kHz, $I(f) < 3 \cdot 10^{-7}/\sqrt{\text{Hz}}$, resulting in frequency noise on the order of $I(f) \cdot \nu_L$, which is negligible.

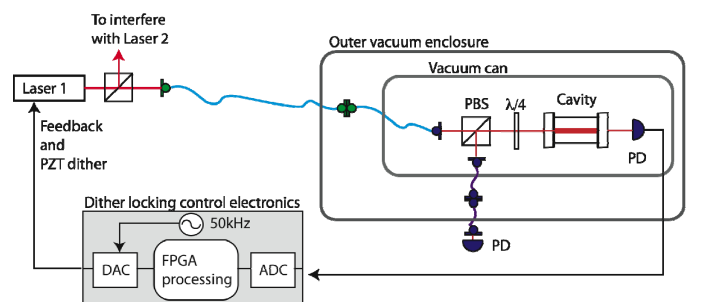


Figure 11. Test configuration using frequency modulation and transmitted light.

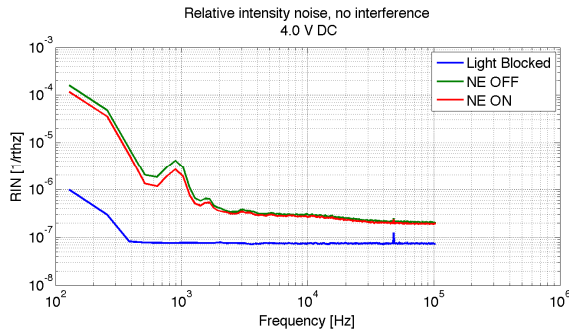


Figure 12. Laser intensity noise with and without built-in "Noise Eater" (NE) intensity stabilization

The same analog-to-digital converters and FPGA system for locking lasers to the cavities was used as in the Pound-Drever-Hall technique. The resulting frequency stability performance is shown in Figure 10. The resulting spectrum has more of a $1/f$ behavior at frequencies below 1 Hz, which indicates a reduction in the effect of stray interference. The $1/f$ behavior is characteristic of thermal fluctuations. The observed $1/f$ power spectrum is higher than expected based on design calculations. This may be due to the vacuum in the cavity enclosure being higher than expected.

D. Adjacent longitudinal mode locking

To ensure that the experiment was not limited by the locking system (electronics, software, etc), two lasers were locked to adjacent longitudinal modes of a single cavity. This gives a large amount of common-mode rejection of certain noise sources, primarily cavity noise, suppressed to the level of the ratio of the optical frequency to the free spectral range (a suppression factor of $\sim 150,000$ in this case). In turn, this allows the differential noise sources, such as the locking systems, to be measured.

After phase modulation sidebands were imposed, the two laser beams were combined via a fiber beam-splitter. One output of this beam-splitter was coupled into the cavity. The reflected fields were detected as described above. The output from the photoreceiver was electronically split, with separate demodulations at the appropriate sideband frequencies, giving separate error signals with which to feed back to each laser. The stability measurement was made in the same manner as described above. These measurements ruled out readout noise as a dominant contributor to the frequency noise for the case with lasers locked to separate cavities.

E. Environmental testing

One optical cavity assembly was tested using vibration and thermal qualification levels specified for the GRACE mission instruments. No serious problems were found. A minor issue was found during the high end of the thermal qualification test and will be addressed in the planned design update.

V. FUTURE WORK

Further testing of the breadboard cavity assemblies is planned to determine the source of excess frequency noise. One possible source of excess noise is higher than expected thermal

fluctuations due to the pressure in the cavity enclosure being higher than anticipated. This was caused by an unexpectedly high rate of outgassing from the optical fibers. This will be explored using a better external vacuum system and venting the cavity enclosure to the better vacuum system. There is evidence that the multimode fiber used for extraction of light reflected from the cavity has some effect even when transmitted light is used for locking. The light into the multi-mode fiber will be blocked to eliminate that effect.

Following the completion of the performance tests, the cavity assembly design will be updated to address the identified shortcomings. A prototype unit will then be assembled and tested.

ACKNOWLEDGMENT

We thank Timothy Lam for providing the digital Pound-Drever-Hall locking subroutine. This work was sponsored by the NASA Earth Science Instrument Incubator Program. This research was carried out in part at the Jet Propulsion Laboratory, California Institute of Technology, under contract with the National Aeronautics and Space Administration.

REFERENCES

- [1] B. Tapley, J. Ries, J. S. Bettadpur, D. Chambers, M. Cheng, F. Condi, B. Gunter, Z. Kang, P. Nagel, R. Pastor, T. Pekker, S. Poole, F. Wang, "GGM02 - An improved Earth gravity field model from GRACE", *Journal Of Geodesy*, vol. 79, pp. 467-478, 2005.
- [2] C. Dunn, J. Kim, Y. Bar-Sever, S. Desai, B. Haines, D. Kuang, G. Franklin, I. Harris, G. Kruizinga, T. Meehan, S. Nandi, D. Nguyen, T. Rogstad, J. B. Thomas, J. Tien, L. Romans, M. Watkins, S.-C. Wu, S. Bettadpur, W. Bertiger, "Instrument of GRACE", *GPS World*, February 2003.
- [3] P. Touboul, E. Willemonot, B. Foulon and V. Josselin, "Accelerometers for CHAMP, GRACE and GOCE space missions: synergy and evolution", *Boll. Geof. Teor. Appl.* vol. 40, pp. 321-327, 1999.
- [4] J. Wahr, S. Swenson, V. Zlotnicki, V. Velicogna, "Time-variable gravity from GRACE: First results", *Geophysical Research Letters* vol. 31, Article No. L11501, 2004.
- [5] J.B. Thomas, "An Analysis of Gravity Field Estimation Based on Intersatellite Dual Biased One-Way Ranging" *JPL Pub.* 98-15 May 1999, p B-3.
- [6] M. Stephens, R. Craig, J. Leitch, and R. Pierce, R.S. Nerem, P. Bender, and B. Loomis, "Interferometric Range Transceiver for Measuring Temporal Gravity Variations", *proceedings of the 2006 Earth Science Technology Conference*, College Park, MD, 2006.
- [7] J. Alnis, A. Matveev, N. Kolachevsky, Th. Udem, and T. W. Hänsch, Subhertz linewidth diode lasers by stabilization to vibrationally and thermally compensated ultralow-expansion glass Fabry-Pérot cavities, *Physical Review A* vol. 77, 053809-9, 2008.
- [8] M. Nothcutt, L. S. Ma, J. Ye, J. L. Hall, "Simple and compact 1-Hz laser system via an improved mounting configuration of a reference cavity", *Optics Letters*, vol. 30, pp. 1815-1817, 2005.
- [9] D. Bortoluzzi, P. Bosetti, L. Carbone, A. Cavalleri, A. Ciccolella, M. Da Lio, K. Danzmann, R. Dolesi, A. Gianolio, G. Heinzl, D. Hoyland, C. D. Hoyle, M. Hueller, F. Nappo, M. Sallusti, P. Sarra, M. Te Plate, C. Tirabassi, S. Vitale and W. J. Weber, "Testing LISA drag-free control with the LISA technology package flight experiment", *Class. Quantum Grav.*, vol. 20, pp. S89-S97, 2003.
- [10] P. Marchetti, J. Blandino, M. A. Demetriou, "Electric Propulsion and Controller Design for Drag-Free Spacecraft Operation", *Journal Of Spacecraft And Rockets*. vol. 45, pp. 1303-1315, 2008.

- [11] D. N. Wiese, W. M. Folkner, R. S. Nerem, "Alternative mission architectures for a gravity recovery satellite mission", *Journal Of Geodesy*, vol. 83, pp. 569-581, 2009.
- [12] N. Sneeuw, J. Flury, R. Rummel, "Science requirements on future missions and simulated mission scenarios", *Earth Moon Planets*, vol. 94, pp. 113-142, 2005.
- [13] D. N. Wiese, "Alternative Mission Architectures for a Gravity Recovery Satellite Mission, Master's Thesis, University of Colorado, 2007.
- [14] B. Nemati, G. M. Kuan, "Model validation of SIM external metrology at the sub-nanometer level, proceedings of SPIE conference on Astronomical Telescopes and Instrumentation, Glasgow, Scotland, United Kingdom, June 21-25, 2004.
- [15] K. Numata, A. Kemery, J. Camp, "Thermal-noise limit in the frequency stabilization of lasers with rigid cavities", *Physical Review Letters*, vol. 93, Article Number: 250602, 2004.
- [16] T. J. Kane and R. L. Byer, "Monolithic, unidirectional single-mode ring laser", *Opt. Lett.*, vol. 10, pp. 65-67, 1985.
- [17] B. Ware, W. M. Folkner, D. Shaddock, R. Spero, P. Halverson, I. Harris, T. Rogstad, "Phase Measurement System for Inter-Spacecraft Laser Metrology, proceedings of the 2006 Earth Science Technology Conference, College Park, MD, 2006.
- [18] D. Shaddock, B. Ware, P. G. Halverson, R. E. Spero, and B. Klipstein, "Overview of the LISA Phasemeter", 6th International LISA Symposium, AIP Conference Series, vol. 873, pp. 654-660, 2006.
- [19] R. W. P. Drever, J. L. Hall, F. V. Kowalski, J. Hough, G. M. Ford, A. J. Munley, and H. Ward, "Laser phase and frequency stabilization using an optical resonator", *Appl. Phys. B*, vol. 31, pp. 97-105, 1983.
- [20] T. T-Y. Lam, S. Chua, B. J. J. Slagmolen, J. H. Chow, I. C. M. Littler, D. E. McClelland and D. A. Shaddock, "A Comparison Between Digital and Analog Pound-Drever-Hall Laser Stabilization", *Proceedings of Conference on Quantum Electronics and Laser Science*, Baltimore, MD, 2-4 June 2009 Location: Baltimore, MD, USA